EMAS Engineering Modelling, Analysis & Simulation THE NAFEMS JOURNAL

NAFEMS

Vol. 2, Issue 1, 2025

Damping coefficients by experiments and the application to transient FE analyses of cable trays

Jack Reijmers[a,1], Alessandro Zambon[a]

[a]Nevesbu B.V., Kelvinring 48, 2952 BG Alblasserdam, The Netherlands

Abstract

Damping entails significant effects in transient analyses, and neglecting it to obtain a conservative solution in numerical analyses might return no meaningful results. For steel structures, dimensionless damping coefficients around 1% of the critical damping are widely accepted. However, for structures consisting of several materials, damping coefficients may be higher; estimating their values reliably is important. This paper studies the case of damping estimates for steel trays supporting cable bundles. Free vibration signals were experimentally acquired using a steel beam with and without attached cables, by employing a smartphone app set to record acceleration data. The logarithmic decrements calculated from the signals resulted in different dimensionless damping coefficients for correspondingly different numbers of cables attached to the beam; five configurations were tested, up to twenty cables on the beam. The resulting damping coefficients showed an increase from 0.7% (without cables and consistent with the usual 1% value) to 3% (with twenty cables). These results were applied to a Finite Element (FE) model of a ladder-type cable tray, subjected to a shock pulse as excitation. Thus, the transient response was investigated for different cases from nearly zero damping up to a 3% level. With negligible damping, the analysis did not converge; instead, with the damping coefficients resulting from the experiment, realistic numerical results were found. It is therefore shown that valuable information could be obtained through a simple experimental setup. Multi-material structures can be easily tested, in order to obtain results that can constitute better input for transient FE analyses.

Keywords

Damping, Experimental setup, Shock response, Cable trays, FE transient analysis

1 Introduction

Cable trays are structural elements that play an essential role in large facilities and ships, as their electrical grids inevitably need cables to be conveyed across different and distant spaces to serve the multiple nodes composing the grids. Seismic loading represents the most significant type of excitation that threatens cable trays' integrity [1]; correspondingly, the continuation of operations via the supported electrical cables is also put at risk. Reliable modelling of the dynamic properties of cable trays is therefore important to correctly design them and ensure compliance with the safety requirements that are needed. Generally, the term "cable tray" refers to the assembly including the cable structure where the cable lay and the supporting components that interface the tray to the surrounding structure. The supporting components can be of various types, and studies have been carried out to investigate their dynamic behaviour, with a particular focus on their damping properties [2], [3], [4]. Besides, experimental studies were conducted to evaluate cable trays' strength and failure patterns [5], [6]; shock tables were employed to test the cable trays. Most of the available literature on the topic of cable tray dynamic response is related to earthquake excitation, thus for civil and industrial building applications. Naval vessels and marine structures are instead exposed to underwater explosions, collisions, and

[1]Corresponding author.
E-mail address: j.j.reijmers@nevesbu.com (J. Reijmers)
https://doi.org/10.59972/rysnhh6t

phenomena causing high acceleration pulses. Although seismic excitation patterns may be analogous, little focus is dedicated to ship and offshore structures' applications; indeed, the design of cable tray systems for marine applications differs from the cable tray design for buildings, as the space constraints, safety requirements, and functionality challenges are different [7]. This entails separate considerations for the trays' supports damping characterization and simulation choices.

A widely accepted idea is that damping has a beneficial effect on the outcome of transient analyses. This implies that ignoring damping must give conservative results. However, it is also possible that the transient analysis, after the initial load, does not deliver the expected free vibration motion. Therefore, in those cases, some damping must be considered in order to correctly simulate the energy dissipation occurring inside the model.

This may result in a stable analysis, but the question remains whether the applied damping coefficient is realistic or not. For steel structures, a dimensionless damping of 1% of the critical damping is usually deemed appropriate. In the study by Hirose et al. [2], the value 0.5% was used instead. However, in the case when a combination of several materials is in place, a realistic value for damping is not readily available, and damping coefficients can be established through experimental data.

As a case study for the present paper, a metallic cable tray subjected to a shock load is considered. An arbitrary low value for damping was initially applied to a FE model of the cable tray; the corresponding transient analysis failed after the shock load has vanished. No stable free vibration resulted from the simulation, and at a certain load step the analysis did not converge. With 1% of the critical damping the analysis showed realistic results, but for this model 1% is questionable. The steel structure is merely a container for cables with a metallic core and composite insulation, and the expected damping coefficients for cables, in particular a pack of cables that contribute to the system's physical properties, must be higher. In fact, a cable tray with bundles of cables fastened to it can be considered as a composite-material structure.

With a simple setup, consisting of general available equipment, free vibration of a steel beam was registered, and the decrease of the motion amplitude led to obtain the logarithmic decrement followed by the dimensionless damping coefficient. In addition, an increasing number of cables was attached to the steel beam, thereby entailing a decreasing natural frequency and an increasing damping coefficient.

These damping coefficients were applied in the FE transient analyses, and the results showed a damped response as expected. It must be noted that the experiments are not a realistic representation of the cable tray subjected to a shock load. However, the focus should be on the effect of a cable pack combined with metallic structures concerning damping, in order to obtain more realistic damping coefficients than the accepted value for steel structures.

A description of the cable tray model is given in Section 2. Basic theory on damping can be found in Section 3. Section 4 presents the layout of the free vibration experiment and an overview of the dimensionless damping coefficients following from an increasing number of cables attached to the beam. Application of these damping coefficients to the FE analysis can be found in Section 5, followed by the conclusions.

2 FE model of the cable tray

The cable tray case study considered in this paper is based on a commercially available model, namely a VC-60 (Niedax) [8]. The FE model that simulates this cable tray is presented in Figure 1.

The FE software tool ANSYS has been used to develop the analysis. Reference is made to the element library and the command reference [9]. The cable tray is modelled with BEAM188 elements. These elements with 2 nodes are applied with the option for unrestrained warping, Poisson effect and a quadratic shape function over the length. The legs are modelled with a hollow rectangular cross section and an element size following from 25 elements between the rungs. The rungs are modelled with a channel cross section and 20 elements over the rung length. The cable mass is distributed over the rungs by using MASS21 elements. With 20 beam elements over a rung each rung carries 19 mass elements. Cable tray supports are modelled by COMBIN14 elements. These 2-node elements contain a damper and a spring. The damper has a damping coefficient defining viscous damping, i.e., damping is proportional to the velocity. The width of the cable tray is 0.20 m, with a distance between the rungs of 0.25 m. The cable tray is supported at 8 locations with a distance in longitudinal direction of 1.20 m. The total length of the model amounts to 4 times the support distance, thus giving 4.80 m overall.

This results in a mass of 13.63 kg. The cable mass is given by 50 kg/m resulting in 240 kg. The total mass (240 + 13.63 = 253.63 kg) is distributed over 8 locations giving 31.70 kg for each support point.

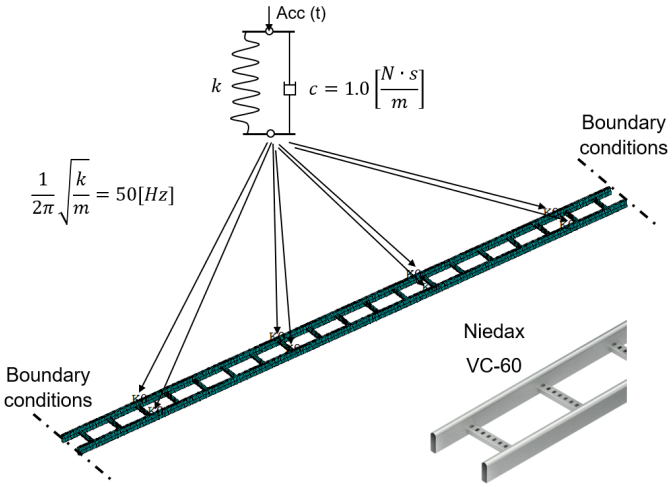

Figure 1. Outline of the FE model of the VC-60 cable tray.

As indicated in Figure 1 the support of the cable tray consists of spring-damper elements (COMBIN14). Each element carries a mass of 31.7 kg, and stiffness of the support shall result in a natural frequency of 50 Hz (or $\omega_n = 2\pi \cdot 50 = 314$ rad/s). This gives:

$$\omega_n = \sqrt{\frac{k}{m}} \quad \rightarrow \quad k = 314^2 \cdot 31.7 = 3.129 \cdot 10^6 \; N/m \tag{1}$$

This value for the stiffness constitutes the first Real constant of the element COMBIN14. The second constant of the element is the damping coefficient, and for this input an arbitrary value of 1.0 N·s/m is applied. The material model of the cable tray is linear elastic steel with a Young's modulus of $E = 206 \cdot 10^9$ N/m^2, a Poisson ratio of $\nu = 0.30$, and a mass density of $\rho = 7850$ kg/m^3.

The dynamic excitation applied to the cable tray's model consists first in a semi-sinusoidal shock pulse with a time span of 5 ms and an amplitude of 2000 m/s^2. This magnitude (approximately 200g) is a typical value used in industrial and military analyses, representing an idealized shock loading. Through the remaining 25 ms (up to $t = 30$ ms) also a semi-sinusoidal pulse is applied, with amplitude of -400 m/s^2; this excitation pattern ensures that the integral of the acceleration curve through the two semi-sinusoidal phases is equal to zero. This therefore means that the overall velocity enforced to the system at the end of the shock pulse is equal to zero. Figure 2 shows the acceleration profile enforced on the model along the vertical direction.

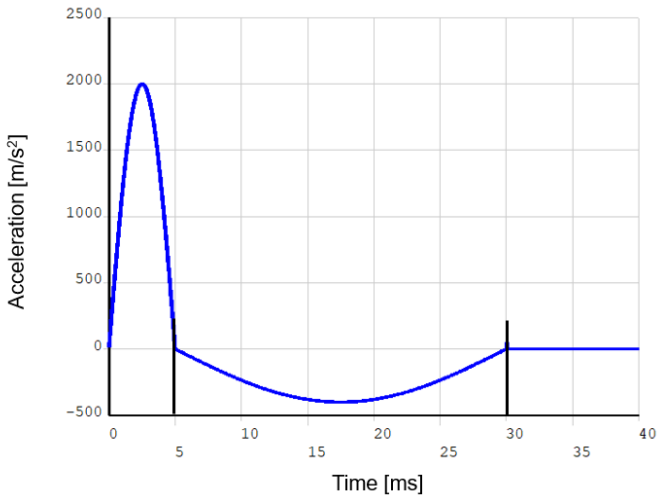

Figure 2. Time plot of the shock excitation applied along the vertical direction.

3 Fundamentals of damping

The FE model shown in Figure 1 represents a system with multiple degrees of freedom, consisting of a mass matrix [*M*], a damping matrix [*C*] and a stiffness matrix [*K*]. This system is excited by a force vector {*F*}(t). With displacement vector {*x*} follows for the motion equation:

$$[M] \cdot \{\ddot{x}\} + [C] \cdot \{\dot{x}\} + [K] \cdot \{x\} = \{F\}(t) \tag{2}$$

Eigenvalue analysis of the homogeneous, undamped system delivers the eigenvectors, contained in the matrix [*X*]. This matrix is used for the transformation to principal coordinates {*p*} [10].

$$\{x\} = [X] \cdot \{p\} \tag{3}$$

Substitution in Equation 2 and pre-multiplication with the transposed matrix [*X*] gives:

$$[X]^T \cdot [M] \cdot [X] \cdot \{\ddot{p}\} + [X]^T \cdot [C] \cdot [X] \cdot \{\dot{p}\} + [X]^T \cdot [K] \cdot [X] \cdot \{p\} = [X]^T \cdot \{F\}(t) \tag{4}$$

The orthogonality of the eigenvectors with respect to mass and stiffness transforms the mass and stiffness matrix, [*M*] and [*K*], to diagonal matrices called principal mass matrix [M_p] and principal stiffness matrix [K_p].

$$[X]^T \cdot [M] \cdot [X] = \left[M_p\right] \; and \; [X]^T \cdot [K] \cdot [X] = \left[K_p\right] \tag{5}$$

Unfortunately, the transformation to principal coordinates will not result in a diagonal damping matrix. However, this problem can be solved by considering the damping matrix proportional to the mass and stiffness matrix.

$$[C] = \alpha \cdot [M] + \beta \cdot [K] \rightarrow [X]^T \cdot [C] \cdot [X] = \alpha \cdot \left[M_p\right] + \beta \cdot \left[K_p\right] \tag{6}$$

The transformation to the principal coordinates *{p}* results in diagonal matrices, and this entails in obtaining uncoupled equations of motion.

$$\left[M_p\right] \cdot \{\ddot{p}\} + \alpha \cdot \left[M_p\right] \cdot \{\dot{p}\} + \beta \cdot \left[K_p\right] \cdot \{\dot{p}\} + \left[K_p\right] \cdot \{p\} = [X]^T \cdot \{F\}(t) \tag{7}$$

Damping proportional to mass means that the lower eigenmodes are damped less, and damping increases with the higher modes. Observing the response of steel structures on an impact load, shows that higher modes damp out quickly and free vibration continues in the lowest eigenmode. This indicates that damping is not proportional to mass (a = 0) but to stiffness (b ≠ 0). This is illustrated in Figure 1, where the dashpot is parallel to the spring.

The free vibration in the lowest eigenmode with b (also called structural) damping is given by:

$$M_{p1} \cdot \ddot{p}_1 + \beta \cdot K_{p_1} \cdot \dot{p}_1 + K_{p1} \cdot p_1 = 0 \tag{8}$$

M_{p1} and K_{p1} are the first elements in the diagonal matrices and p_1 the first element in the vector with principal coordinates.

The natural frequency of this (undamped) mode follows from:

$$\omega_{n1} = \sqrt{\frac{K_{p1}}{M_{p1}}} \tag{9}$$

The critical damping [11] of this mode is given by:

$$C_{c1} = 2 \cdot \sqrt{K_{p1} \cdot M_{p1}} = 2 \cdot M_{p1} \cdot \omega_{n1} \tag{10}$$

This gives a dimensionless damping coefficient:

$$\xi_1 = \frac{C_{p1}}{C_{c1}} = \frac{\beta \cdot K_{p1}}{2 \cdot M_{p1} \cdot \omega_{n1}} = \frac{\beta \cdot \omega_{n1}}{2} \tag{11}$$

From Equation 11 follows for the structural damping factor:

$$\beta = \frac{\xi_1 \cdot \omega_{n1}}{2} \tag{12}$$

In fact, the transformation to principal coordinates makes the matrices diagonal, and this results in a set of decoupled motion equations. This implies that each mode represents a single degree of freedom system.

The first analysis considers the cable tray with the cables modelled as a rigid mass, and this reduces the model to a single degree of freedom system with motion equation:

$$m \cdot \ddot{x} + c \cdot x + k \cdot \dot{x} = f(t) \tag{13}$$

The mass (m = 31.7 kg) and stiffness (k = 3.129·10^6 N/m) determine the critical damping, as presented in Equation (10), and this value follows from:

$$c_c = 2 \cdot \sqrt{k \cdot m} = 2 \cdot \sqrt{3.129 \cdot 10^6 \cdot 31.7} = 1.992 \cdot 10^4 \; N \cdot s/m \tag{14}$$

As stated above, an arbitrary damping coefficient $c = 1.0$ N·s/m is applied, and this input gives a dimensionless damping coefficient (ξ):

$$\xi = \frac{c}{c_c} = \frac{1.0}{1.992 \cdot 10^4} = 5.020 \cdot 10^{-5} \tag{15}$$

DNVGL [12] presents damping values for structures subjected to environmental loads, and in case of vortex shedding a suggested value is x = 0.0015. For pure steel pipes in water DNVGL presents a value of 0.005 and the damping coefficient increases to 0.03 to 0.04 for flexible pipes. For more information DNVGL refers to Blevins [13]. This book contains a table with a summary of damping tests for several structures. The minimum tested value in [13] is 0.0016 for steel towers.

More data on damping are presented by Adams and Askenazi [14]. For continuous metal structures a damping value between 0.02 and 0.04 is given and for metal structures with joints this value increases between 0.03 and 0.07.

From this overview follows clearly that the arbitrary input for the FE model in Figure 1, c = 1.0 N·s/m, results in a nearly undamped system.

4 Damping experiments

For the present work, damping coefficients were determined by free vibration experiments of a cantilever beam setup. A basic wall strip for shelf brackets was used, clamped at one side to the desk and on the other side carrying a smartphone. This experimental setup is shown in Figure 3. The distance between the desk and the plate with the smartphone was about 0.60 m.

By using a motion-recording app on the phone, the output of the acceleration sensor inside was registered. The smartphone app that was employed is named *Physics Toolbox* [16], which records acceleration signals with a sampling frequency of 410 Hz. The app includes the feature of writing the measured time series data into an Excel file, which offers the possibility to post-process the result.

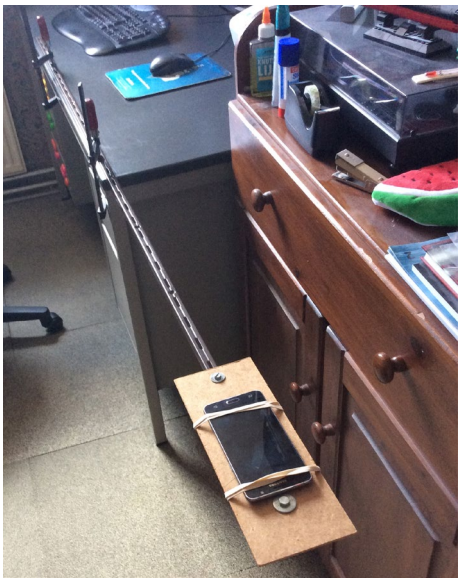

Figure 3. Setup of the free vibration experiment.

Firstly, the Physics Toolbox is tested by a drop experiment. From a height of 2 m the cell phone is released to fall on a soft bed, and the registration of the fall is presented in Figure 4. The registration covering time before release and after contact is presented in Figure 4.a with a narrower time interval

in Figure 4.b. The vertical axis shows g-force, and up to a time t = 5.87 s the acceleration acting on the cell phone is 1.0 g (9.81 m/s2). At that time the phone is released, and the gravity acceleration decreases to zero, as expected in a free fall.

It is emphasized that this test is intended to verify the values presented at the vertical axis of the registration. However, the time axis offers an estimation of the time to contact. To prevent damage to the phone, a soft bed is used, and this makes it difficult to mark a sharp time of contact. Furthermore, a free fall implies the absence of resistance but the flow of air around the falling phone will raise a force. Ignoring this effect and taking a free fall over 2.0 m by an acceleration of 9.81 m/s^2 results in a time:

$$\frac{1}{2} \cdot 9.81 \cdot t^2 = 2.0 \quad \rightarrow \quad t = 0.64\ s$$

This time interval is plotted in Figure 4.b, and the interval ends just before the acceleration peak that indicates the end of the motion downward. This result can be regarded as a validation of the tool, but it must be noted that an accurate value of the acceleration is not required for the free vibration test. This will be demonstrated in the following test.

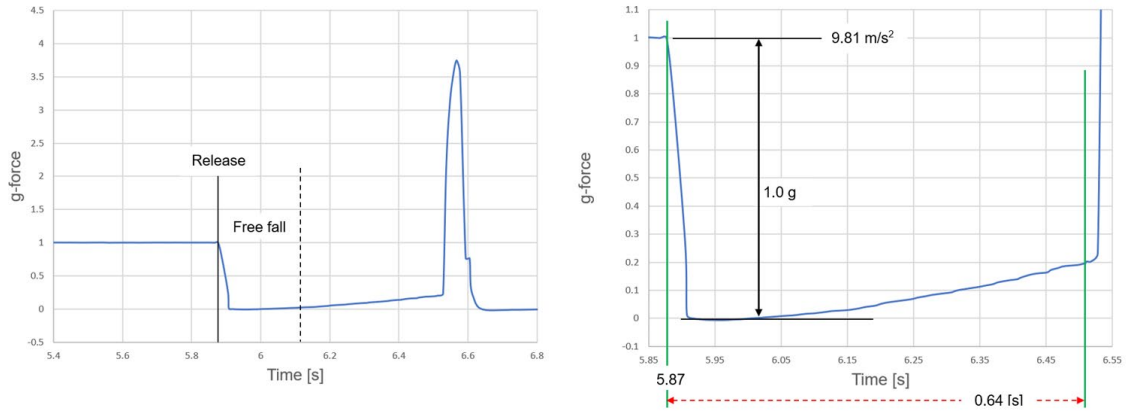

(a) Overview from release to contact (b) Detail of the free-fall segment

Figure 4. Registration of a drop test of the cell phone.

Figure 5 shows the free vibration plot from the saved acceleration data of the configuration with no cables attached to the beam, as shown in Figure 3.

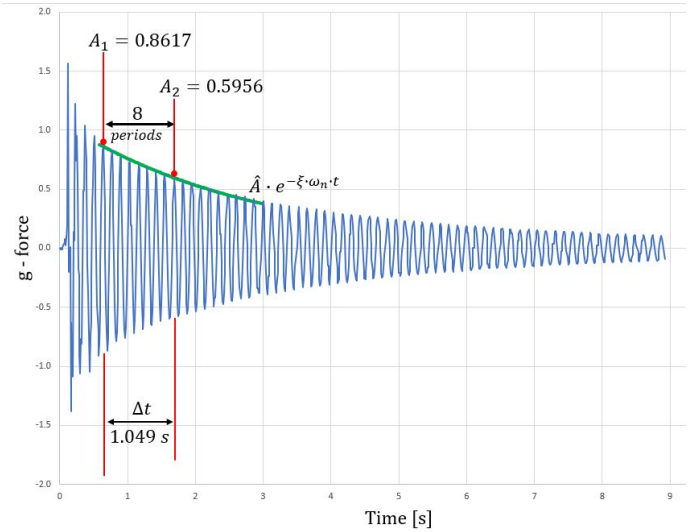

Figure 5. Registration of the free vibration of the beam without cables attached.

Two amplitudes (*g*-force) are measured: $A_1 = 0.8617g$ and $A_2 = 0.5956g$, covering 8 complete periods. The logarithmic decrement is given by the ratio of the amplitudes [11]. The logarithmic decrement results as:

$$\delta = \frac{1}{8} \cdot ln\left(\frac{0.8617}{0.5956}\right) = 0.0462 \tag{16}$$

As stated above, the exact value of the amplitude is of little importance since the test aims at the ratio of the amplitudes under consideration, irrespective of the dimensions.

The time interval over the 8 complete periods results from the measured signals as: $\Delta t = 1.049$ s; this value gives a period equal to:

$$\tau = \frac{1.049}{8} = 0.131\ s \tag{17}$$

With the dimensionless damping coefficient ξ and natural frequency ω_n, the relation between logarithmic decrement δ and the period τ is given by:

$$\delta = \xi \cdot \omega_n \cdot \tau \tag{18}$$

The period τ is slightly influenced by the damping according to the following equation:

$$\tau = \frac{2\pi}{\omega_n \cdot \sqrt{1 - \xi^2}} \tag{19}$$

However, with the actual small damping coefficients the term under the square root can be approximated to 1, therefore the period can be expressed by the natural period for undamped vibration:

$$\tau \approx \tau_n = \frac{2\pi}{\omega_n} \tag{20}$$

By using Equations (16) and (18), this finally leads to the value for the dimensionless damping coefficient:

$$\delta = 2\pi \cdot \xi \quad \Longrightarrow \quad \xi = \frac{\delta}{2\pi} = \frac{0.0462}{2\pi} = 0.0073 \tag{21}$$

The natural frequency follows from:

$$\omega_n = \frac{2\pi}{\tau} = \frac{2\pi}{0.131} = 47.9 \frac{rad}{s} \quad or\ f_n = \frac{1}{\tau} = 7.63\ Hz \tag{22}$$

Figure 6 shows the situation with 20 cables attached to the beam, and the corresponding free vibration registration is displayed in Figure 7.

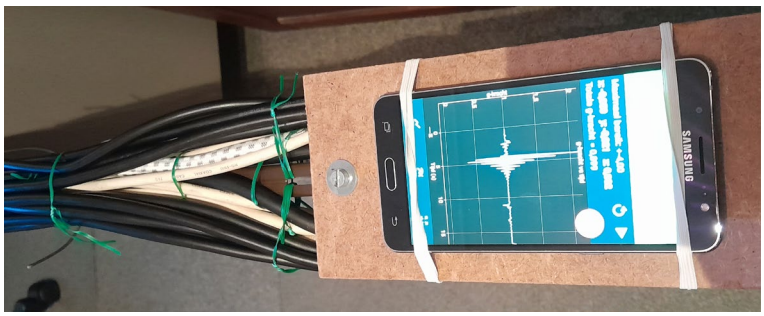

Figure 6. Setup for the experiment with 20 cables attached to the beam.

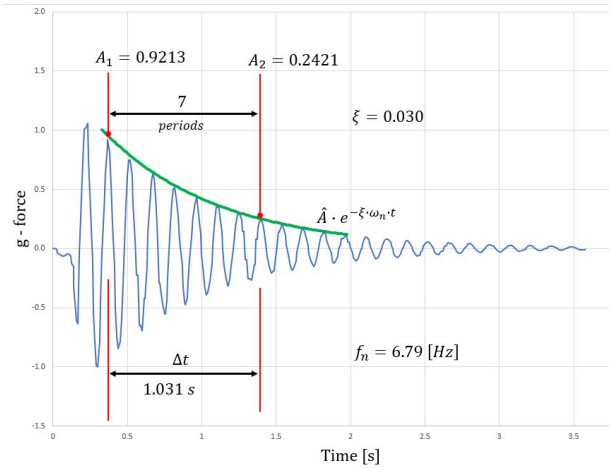

Figure 7. Motion signal's registration of the free vibration of the beam with 20 cables.

This registration leads to a logarithmic decrement followed by the dimensionless damping coefficient. Namely:

$$\delta = \frac{1}{7} \cdot ln\left(\frac{0.9213}{0.2421}\right) = 0.1909 \; and \; \xi = \frac{\delta}{2\pi} = \frac{0.1909}{2\pi} = 0.030$$

The damping values retrieved from the experiments with other cable packs are listed in Table 1. The damping coefficient ξ increases from 0.007 for the case of the plain beam to 0.030 for the beam carrying 20 cables. This means that the influence of the full cable pack entails a 4.3 factor between the damping coefficients of the two extreme cases.

Table 1. Overview of the results following from the experiments.

Number of cables on the beam	Logarithmic decrement, δ	Damping coefficient, ξ
0	0.04617	0.007
2	0.07110	0.011
8	0.11738	0.019
14	0.17087	0.027
20	0.19092	0.030

The influence of the cables on the actual entity of the composite system's damping is clearly demonstrated. It is then justified to apply to the model a value of 3% of the critical damping when cable trays are filled with cables.

5 Application of damping in the transient analysis

When using the damping ratio as per Equation 16, the dynamic simulation of the system under the shock excitation (Figure 2) produces unrealistic outcomes due to bad convergence of the numerical solver. The result is shown in Figure 8: initially, the response looks like a free vibration oscillation with a very slowly decreasing amplitude; beyond the duration of the shock pulse excitation ($t > 30$ ms), the response does not decay to zero, but instead it deranges to unplausible values. At $t = 81$ ms, the simulation gets aborted due to convergence impossibility.

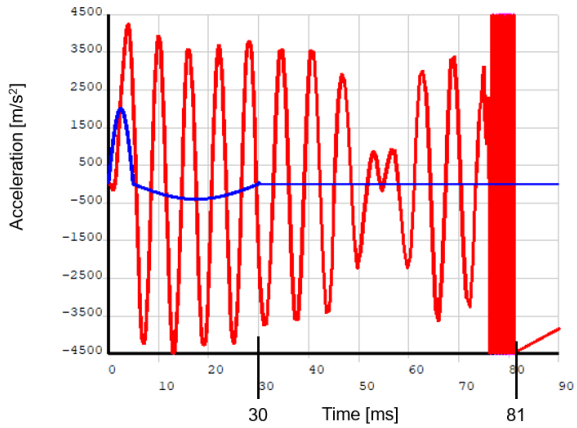

Figure 8. Response of the FE model when applying a damping ratio of ξ = 5.02E-5.

The values presented in Table 1 for the dimensionless damping coefficient ξ produce in combination with Equation (11) the damping values for the spring-damper elements (*COMBIN14*). In addition, the structural damping in Equation (12) is modelled in ANSYS through the command *BETAD*.

The modified input by using $\xi = 0.007$ to 0.030 entails a stabilization of the response of the system to the shock pulse, thus with an actual decay of the motion amplitude after the end of the shock excitation. Figure 9 shows the model's relative displacement responses (blue curve, namely the motion difference between two nodes positioned laying at the two different sides of the cable tray), which visibly decay to zero after the positive pulse of the enforced acceleration. On the top of Figure 9, the response obtained with $\xi = 0.007$ is shown; this value corresponds to the scenario with no cables attached to the beam, according to the experimental outcome shown in Table 1. Also in this case, attenuation of the oscillating response can be noticed, although with a significantly lower energy dissipation due to the lower

damping, as expected. The numerical solver therefore demonstrated to converge when these damping settings are adopted.

Besides, it can be observed that even a small contribution of damping makes the response significantly attenuated; more specifically, few oscillation cycles and a short time after the shock pulse are sufficient to make the system reach the stationary state again.

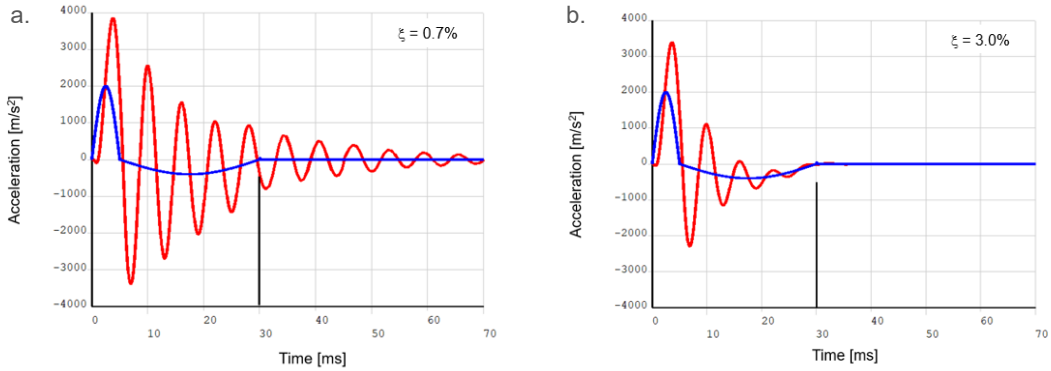

Figure 9.a. Response of the cable tray's FE model (nodes with maximum acceleration) under an equivalent damping ratio of ξ=0.007, and in b. for ξ=0.030 with the corresponding shock pulse excitation displayed.

Figure 10 shows the deformed shape of the cable tray's model at a time step close to $t = 3.7$ ms, namely shortly after passing the positive pulse's peak, which occurs at $t = 2.5$ ms. The positions and constraints of the 8 supports determine the deformed pattern that arises during and after the excitation timespan.

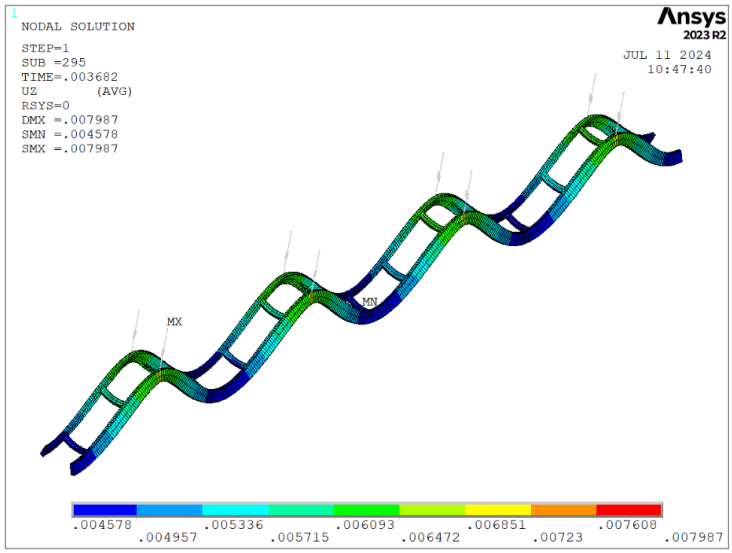

Figure 10. Deformed shape and contour plot of the FE cable tray (magnified).

6 Conclusions

In this paper, the problem of estimating a realistic value for the damping characteristics of cable trays has been considered. We used the outcomes from a simple experimental setup to evaluate the damping coefficient of a steel beam with diverse packs of cables attached to it. A FE model of a commercial cable tray was developed to simulate its transient response to shock loads; the application of the experimental-derived damping information made the FE analysis converge.

It must be noted that the experiments herein presented are not intended to reproduce the actual behaviour of a cable tray. Instead, the experimental setup aims to highlight the effect of cables bundled to a steel beam on the dynamic response of the overall system. The damping coefficient for the steel

beam without cables, namely $\xi = 0.007$, is lower than the usually accepted value for steel structures (1% of the critical damping).

Further work over this study subject could be developed, given the multitude of application of cable trays and their structural variability. The utilization of different types of shock resilient supports can be studied to determine the dynamic response of the trays, also to consider correspondingly different damping formulations in the mathematical model. Besides, having the cable bundles fastened or not to a cable tray is an option that would need to be accounted for, as unfastened cable bundles contribute less to the inertia of the overall system; the problem would thereby transform into a multi-body simulation. Finally, full-scale experiments using actual cable trays should be conducted, in order to test different configurations under shock loads and measure the corresponding full-scale response, which would provide more realistic insights into the actual damping properties of cable trays.

7 References

[1] Z. Fu and S. Wu, “Seismic performance sensitivity analysis to random variables for cable tray system”, in Journal of Civil Engineering and Management, 2024, Vol. 30, Issue 1, pp 85-98

[2] J. Hirose, I. Ichihashi, Y. Horimizu, K. Fujita, Y. Uchiyama, K. Gunyasu, “Study on cable tray damping ratios”, 1988, in Pressure Vessel and Piping Division, Vol, 133, pp 49-54, ASME

[3] H. Jiang and S. Wu, “Theoretical analysis and optimization of toggle-brace damper for cable tray system”, in Journal of Constructional Steel Research, Vol. 187, art. n. 106936, 2021

[4] H. Jiang, W. Huang, S. Wu, C. Wu, “Hysteretic model for main to sub beam joints of cable tray”, 2023, in Journal of Building Engineering, Vol. 72, art. n. 106471, 2023

[5] K. Komatsu, H. Fuyama, K. Imai, K. Myojin, E. Kokubo, “Cable tray ultimate strength test employing a large shaker table”, in the Proceedings of the International Conference on Nuclear Engineering (ICONE12), Vol. 2, pp 233-240, 2004

[6] C. Wu, K. Matsuda, H. Jiang, S. Wu, K. Mizutani, K. Kasai, “Dynamic responses and failure pattern of suspended cable tray system through shaking table test”, in the Report of the IABSE Symposium Prague 2022: Challenges for Existing and Oncoming Structures, pp 662-669, 2022

[7] V. Blanco, G. González, Y. Hinojosa, D. Ponce. M. A. Pozo, J, Puerto, “The pipelines and cable trays location problem in naval design”, in Ocean Engineering, Vol. 286, art. n. 115525, 2023

[8] Niedax, “Product information cable trays”, Accessed 4 September 2024, Website (in Dutch) https://www.niedax.nl/media/34elycer/02_alround_vo_vc_vot.pdf

[9] ANSYS, Inc., Canonsburg, PA 15317, USA, Element & Command Reference, Release 2024 R2, July 2024

[10] S. Timoshenko, D.H. Young and W. Weaver jr., “Principal and normal coordinates”, in Vibration problems in engineering, fourth edition, John Wiley & sons, 1974, chapter 4.3, pp 296

[11] W.T. Thomson, “Damped free vibration”, in Vibration theory and applications, 6th impression. London, Great Britain, George Allen & Unwin, 1978, chapter 2, pp. 37 - 44

[12] DNVGL, “Environmental conditions and environmental loads”, Recommended Practice, DNVGL-RP-C205, Edition September 2019, §9.1.9, pp 185

[13] R.D. Blevins, “Damping of structures”, in Flow-induced vibration, Second edition, Van Nostrand Reinhold, 1990, chapter 8, pp 326 - 338

[14] V. Adams, A. Askenazi, Building better products with Finite Element Analysis

[15] ANSYS, Inc., Canonsburg, PA 15317, USA, Structural Analysis Guide §1.2.1, Release 2024 R2, July 2024

[16] “Physics Toolbox”. Vieyra Software. Available at https://www.vieyrasoftware.net/